Fast Array Response Adjustment With Phase-Only Constraint: A Geometric Approach

Xuejing Zhang, *Student Member, IEEE*, Zishu He, *Member, IEEE*, Bin Liao, *Senior Member, IEEE*, and Xuepan Zhang

***Abstract*— This paper presents a geometric approach to fast array response adjustment with phase-only constraint. The devised algorithm can precisely and rapidly adjust the array response of a given point by only tuning the excitation phases of a preassigned weight vector. We geometrically reformulate the phase-only array response adjustment as a polygon construction problem, which can be solved by edge rotation in the complex plane. On this basis, we carry out a detailed analysis of the solution of polygon construction and specify the range of the feasible phase. To avoid the undesirable pattern distortion and obtain less pattern variations in the uncontrolled region, an effective and analytical phase determination approach is presented. The proposed algorithm provides an analytical solution and guarantees a precise phase-only adjustment without pattern distortion. In addition, our algorithm does not impose any restriction on the given weight vector and has a low computational complexity. Representative examples are presented to demonstrate the effectiveness of the proposed algorithm under various situations.**

***Index Terms*— Array signal processing, beampattern synthesis, geometric approach, phase-only control.**

I. Introduction

SENSOR arrays have found numerous applications in the field of electromagnetic engineering, and controlling the array power response as desired is of great significance. Quite a number of approaches have been presented to control the array response by finding an appropriate complex-valued weight and designing both amplitudes and phases of excitation for the given specification, see e.g., [2]–[9]. Since each array element requires an amplitude adjustment unit with high dynamic range, the hardware architecture is complicated and high cost is required when implementing these approaches.

To simplify the beamforming network and reduce the cost, phase-only control is preferred [10]–[12]. In the phase-only control, the excitation amplitudes of the array elements are known and fixed as constants (although they may be different from each other), and only the excitation phases can be tuned. The phase-only architecture allows the usage of a single power-divider network, which is more efficient than the traditional architecture where the amplitudes of excitation are modified dynamically [13]. Moreover, the reconfigurability of beampattern can be readily realized with phase shifters in the phase-only architecture, without relying on an additional hardware.

During the past few decades, many phase-only response control and/or pattern synthesis methods have been reported. For reconfigurable conformal arrays, a phase-only power synthesis technique is presented in [14], and an intersection finding problem is formulated and solved by means of the generalized projection algorithm. For linear and planar arrays, the phase-only synthesis of minimum peak sidelobe patterns is considered in [15]. In [16], a computationally efficient approach to phase-only pattern synthesis is proposed using the technique of approximated beam addition, and a direct data domain least squares approach is presented in [17]. An innovative approach is proposed in [18] to synthesize minimally redundant sparse arrays radiating phase-only reconfigurable sum and difference patterns. Kadlimatti and Parimi [19] propose to synthesize the asymmetric radiation patterns for uniformly spaced linear arrays (ULAs) using odd phase excitations. Other classic methods, to name just a few, include successive projection method [20], intersection approach [21], null perturbation algorithm [22], and biquadratic programming method [23].

Taking advantage of advances in convex optimization [24], several new phase-only response control algorithms have been devised. For instance, in [25], the semidefinite relaxation (SDR) technique [26] has been applied for phase-only control. A different convex relaxation (CR) approach is proposed in [27], where the alternating optimization algorithm is adopted to solve the relaxed problem. Note that the resultant patterns of these two algorithms may not meet the original design requirements, since the relaxation operation can only ensure an approximate solution.

Manuscript received January 14, 2019; revised May 20, 2019; accepted May 31, 2019. Date of publication June 20, 2019; date of current version October 4, 2019. This work was supported in part by the National Nature Science Foundation of China under Grant 61671139, Grant 61671137, Grant 61771316, Grant 61701499, and Grant 61871085, in part by the Foundation of Shenzhen under Grant JCYJ20170302150044331, and in part by the China Scholarship Council. This paper was presented in part at the IEEE Radar Conference, Boston, MA, USA, April 22–26, 2019 [1]. *(Corresponding author: Xuepan Zhang.)*

X. Zhang and Z. He are with the School of Information and Communication Engineering, University of Electronic Science and Technology of China, Chengdu 611731, China (e-mail: xjzhang7@163.com; zshe@uestc.edu.cn).

B. Liao is with the Guangdong Key Laboratory of Intelligent Information Processing, Shenzhen University, Shenzhen 518060, China (e-mail: binliao@szu.edu.cn).

X. Zhang is with the Qian Xuesen Laboratory of Space Technology, Beijing 100094, China (e-mail: zhangxuepan@qxslab.cn).

This article has supplementary downloadable multimedia material available at http://ieeexplore.ieee.org provided by the authors. This file contains a MATLAB demo for this work, which is made available for personal purpose. This material is 16 KB in size.

Color versions of one or more of the figures in this article are available online at http://ieeexplore.ieee.org.

Digital Object Identifier 10.1109/TAP.2019.2923083

As a special kind of response control, phase-only nulling for directional interference rejection has also attracted much research interest. In [28], both the theoretical and practical aspects of phase-only weighting for adaptive sidelobe nulling are investigated. By utilizing the first-order approximations and assuming that the phase perturbations are small, an analytical solution is derived in [29] for pattern nulling. Without restricting the size of the phase perturbation, nonlinear programming techniques are used in [30] to realize pattern nulling at the symmetric locations. In [31], the pattern nulling problem is relaxed for arbitrary arrays and solved via semidefinite programming. Apart from the aforementioned methods, there also exist quite a few approaches on adaptive phase-only nulling using neural network [32] and numerical optimization techniques, such as genetic algorithm (GA) [33], bat algorithm (BA) [34], random search [35], steepest descent [36], and conjugate gradient or Newton's method [37]. Usually, numerical optimization approaches may suffer from prohibitive computational complexity. Moreover, their resulting solutions may be trapped into a local minimum far from satisfaction.

It is worth noting that, in general, the aforementioned methods in [24]–[37] lack flexibility in array response control. More specifically, the weight vector design procedure needs to be completely reconducted, even if a slight change (e.g., the response level at one specific direction) of the desired beampattern is made. This makes the traditional approaches inflexible and impractical, especially in the case, when burst interference or signal exists and requires a swift suppression or reception. The above imperfections of the existing approaches motivate us to develop a novel fast array response adjustment algorithm with phase-only constraint, which considers the problem of how to rapidly control the array response at a given direction by only adjusting the phase excitations.

In this paper, a geometric formulation to the problem of phase-only array response adjustment is developed based on the geometric approach [38]. It is shown that the one-point phase-only response adjustment can be alternatively realized by polygon construction in the complex plane. According to this observation, we give a detailed analysis on the feasibility of phase-only adjustment problem and then specify the range of the feasible phases one-by-one. To obtain a solution which causes small pattern variations at the unadjusted region, we propose to set the ultimate phase as the one closest to the corresponding phase of a predesigned weight vector with desirable beampattern. The proposed algorithm provides an analytical solution and guarantees a precise phase-only adjustment without pattern distortion. Moreover, for the given array response adjustment task at a given direction, we design a new weight with the assistance of the previous one, thus avoiding the complete redesign and making the proposed method more flexible. Our algorithm is able to realize rapid array response adjustment with a low computational complexity for any given weight vectors. Representative examples are presented to demonstrate the effectiveness of the proposed algorithm under various situations.

The rest of the paper is organized as follows. In Section II, the problem formulation of phase-only array response adjustment is introduced and the devised algorithm is presented. In Section III, we carry out extensive numerical examples to validate the excellent performance of the proposed algorithm. Conclusions are drawn in Section IV.

Notations: We use bold upper case and lower case letters to represent matrices and vectors, respectively. $j \triangleq \sqrt{-1}$. $(\cdot)^{\mathrm{T}}$ and $(\cdot)^{\mathrm{H}}$ denote the transpose and Hermitian transpose, respectively. $|\cdot|$ is the absolute value and $\|\cdot\|_2$ denotes the l_2 norm. $\Re(\cdot)$ and $\Im(\cdot)$ denote the real and imaginary parts, respectively. $\mathbf{P}_{\mathbf{Z}}$ and $\mathbf{P}_{\mathbf{Z}}^{\perp}$ represent the projection matrices onto the column space of $\mathbf{Z}$ [denoted as $\mathcal{R}(\mathbf{Z})$] and the orthogonal complementary space of $\mathcal{R}(\mathbf{Z})$ [denoted as $\mathcal{R}^{\perp}(\mathbf{Z})$], respectively. $\odot$ denotes the element-wise product operator. $\angle(\cdot)$ outputs phase of the input. $(\cdot)_{2\pi}$ is the mod 2π operation, i.e., it returns to the remainder after division of input by 2π. Finally, we use $\overrightarrow{v_n}$ to denote a 2-D vector in the complex plane, whose coordinate is given by $[\Re(v_n), \Im(v_n)]$.

II. Proposed Algorithm

A. Geometric Interpretation of Phase-Only Array Response Adjustment

We consider an array of $N \geq 3$ elements and aim to vary the entry phases of a given weight vector $\mathbf{w}_{\mathrm{pre}}$ such that the resulting new weight vector $\mathbf{w}_{\mathrm{new}}$ adjusts the normalized array power response at a preassigned angle θ_c to its desired level ρ_c, i.e.,

$$L_{\mathrm{new}}(\theta_c, \theta_0) \triangleq \frac{\left|\mathbf{w}_{\mathrm{new}}^{\mathrm{H}}\mathbf{a}(\theta_c)\right|^2}{\left|\mathbf{w}_{\mathrm{new}}^{\mathrm{H}}\mathbf{a}(\theta_0)\right|^2} = \rho_c \tag{1}$$

where θ_0 represents the main beam axis, $\mathbf{a}(\theta)$ stands for the steering vector at θ, and the nth entries of $\mathbf{w}_{\mathrm{new}}$ and $\mathbf{w}_{\mathrm{pre}}$ (denoted by $w_{\mathrm{new},n}$ and $w_{\mathrm{pre},n}$, respectively) fulfill the condition

$$w_{\mathrm{new},n} = |w_{\mathrm{pre},n}| \cdot e^{j\phi_n}, \quad n = 1, \ldots, N \tag{2}$$

with $\phi_n = \angle w_{\mathrm{new},n}$. By introducing a phase parameter $\psi_c \in [0, 2\pi)$, we can eliminate the quadratic form in (1) and rewrite (1) as

$$\frac{\mathbf{w}_{\mathrm{new}}^{\mathrm{H}}\mathbf{a}(\theta_c)}{\mathbf{w}_{\mathrm{new}}^{\mathrm{H}}\mathbf{a}(\theta_0)} = \sqrt{\rho_c}e^{j\psi_c} \tag{3}$$

or equivalently

$$\mathbf{w}_{\mathrm{new}}^{\mathrm{H}} \underbrace{\left(\mathbf{a}(\theta_c) - \sqrt{\rho_c}e^{j\psi_c}\mathbf{a}(\theta_0)\right)}_{\triangleq \mathbf{h}(\theta_c, \theta_0, \rho_c, \psi_c)} = \sum_{n=1}^{N} h_n |w_{\mathrm{pre},n}| e^{-j\phi_n} = 0 \tag{4}$$

where h_n denotes the nth entry of $\mathbf{h}(\theta_c, \theta_0, \rho_c, \psi_c)$. How to select the phase ψ_c will be presented later in Section II-D, and we assume in the following discussion that ψ_c is known. Given θ_c, θ_0, ρ_c, and ψ_c, our concern is finding the appropriate ϕ_n, $n = 1, \ldots, N$, to satisfy (4).

For notational simplicity, let us define

$$v_n \triangleq h_n \cdot |w_{\mathrm{pre},n}|, \quad n = 1, \ldots, N \tag{5}$$

then we can rewrite (4) as $\sum_{n=1}^{N} v_n e^{-j\phi_n} = 0$. In a view of the complex plane, $v_n e^{-j\phi_n}$ corresponds to a vector, denoted as $\overrightarrow{v_n e^{-j\phi_n}}$, whose coordinate is given by

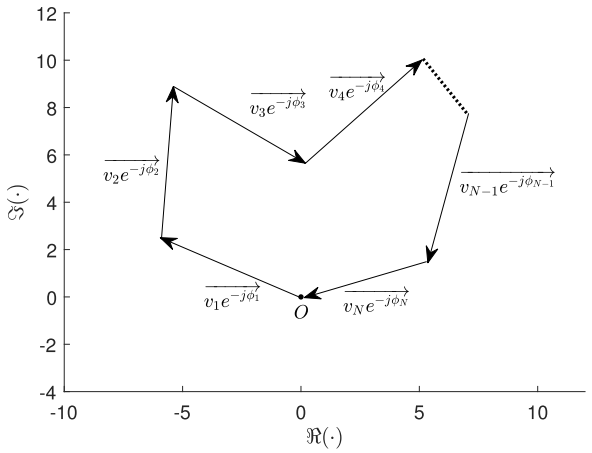

Fig. 1. Geometric illustration of (6).

$[\Re(v_ne^{-j\phi_n}), \Im(v_ne^{-j\phi_n})]$. With this geometric concept, one can denote (4) as

$$\sum_{n=1}^{N} \overrightarrow{v_ne^{-j\phi_n}} = \sum_{n=1}^{N} \overrightarrow{|v_n|e^{j(\vartheta_n-\phi_n)}} = \overrightarrow{\mathbf{0}} \tag{6}$$

where $\vartheta_n = \angle v_n = \angle h_n$, $n = 1, \ldots, N$. The problem of solving (4) with respect to ϕ_n rests on how to rotate the vectors $\overrightarrow{v_n}$, $n = 1, \ldots, N$, in the complex plane to sum them up to a zero vector, as demonstrated in Fig. 1. As a matter of fact, this is equivalent to constructing a polygon with edges $|v_n|$, $n = 1, \ldots, N$, see e.g., [38].

B. Geometric Solution via Triangle Construction

We now investigate the feasibility of (6) and present a solution via triangle construction [38]. To begin with, let us define a permutation matrix $\mathbf{J}$ which sorts $|v_1|, \ldots, |v_N|$ in descending order as

$$[d_1, \ldots, d_N]^{\mathrm{T}} = \mathbf{J}[|v_1|, \ldots, |v_N|]^{\mathrm{T}} \tag{7}$$

where $d_1 \geq d_2 \geq \ldots \geq d_N > 0$. With the above notation, one can readily learn that solving problem (6) with respect to ϕ_n is equivalent to finding $\{\varphi_1, \ldots, \varphi_N\}$ such that

$$\sum_{i=1}^{N} \overrightarrow{d_ie^{j\varphi_i}} = \overrightarrow{\mathbf{0}}. \tag{8}$$

Obviously, the mapping between ϕ_n and φ_n is given by

$$[\phi_1, \ldots, \phi_N]^{\mathrm{T}} = [\vartheta_1, \ldots, \vartheta_N]^{\mathrm{T}} - \mathbf{J}^{\mathrm{T}}[\varphi_1, \ldots, \varphi_N]^{\mathrm{T}} \tag{9}$$

where the fact that $\mathbf{J}^{-1} = \mathbf{J}^{\mathrm{T}}$ is used. As a consequence, the determination of ϕ_n, $n = 1, \ldots, N$, depends on solving (8) with respect to φ_i, $i = 1, \ldots, N$. Before proceeding, we present the following lemma [38].

Lemma 1: Assume $d_1 \geq d_2 \geq \ldots \geq d_N > 0$ and define a piecewise summation function $Q(\cdot)$ as

$$Q(k, l) \triangleq \sum_{i=k}^{l} d_i, \quad 1 \leq k \leq l \leq N. \tag{10}$$

Then if

$$d_1 \leq Q(2, N) \tag{11}$$

we have

$$d_1 \geq \min_{i\in\{2,\ldots,N-1\}} |Q(2, i) - Q(i + 1, N)|. \tag{12}$$

Proof: See [38]. ∎

On the basis of Lemma 1, the following important corollary can be obtained.

Corollary 1: If $d_1 \leq Q(2, N)$, the nonlinear (8) has the following solution as:

$$\varphi_i = \begin{cases} \pi, & \text{if } i = 1 \\ \alpha_1, & \text{if } 2 \leq i \leq m \\ \alpha_1 + \alpha_2 + \pi, & \text{if } m + 1 \leq i \leq N \end{cases} \tag{13}$$

where m is the index satisfying

$$m = \arg \min_{i\in\{2,\ldots,N-1\}} |Q(2, i) - Q(i + 1, N)| \tag{14}$$

α_1 and α_2 are given by

$$\alpha_1 = \operatorname{acos}\left(\frac{d_1^2 + Q^2(2, m) - Q^2(m + 1, N)}{2d_1Q(2, m)}\right) \tag{15a}$$

$$\alpha_2 = \operatorname{acos}\left(\frac{Q^2(2, m) + Q^2(m + 1, N) - d_1^2}{2Q(2, m)Q(m + 1, N)}\right). \tag{15b}$$

Proof: Given the m in (14), if (11) is satisfied, i.e.

$$d_1 \leq Q(2, N) = Q(2, m) + Q(m + 1, N) \tag{16}$$

we can obtain from Lemma 1 that

$$d_1 \geq |Q(2, m) - Q(m + 1, N)|. \tag{17}$$

This indicates that the three edges, i.e., d_1, $Q(2, m)$ and $Q(m+1, N)$, can form a triangle[1] as shown in Fig. 2, where α_1 denotes the included angle between the edges d_1 and $Q(2, m)$, and α_2 is the included angle between the edges $Q(2, m)$ and $Q(m+1, N)$. The specific expressions of α_1 and α_2 are given by (15). In a geometric manner, we have

$$\overrightarrow{d_1e^{j\pi}} + \overrightarrow{Q(2, m)e^{j\alpha_1}} + \overrightarrow{Q(m + 1, N)e^{j(\alpha_1+\alpha_2+\pi)}} = \overrightarrow{\mathbf{0}} \tag{18}$$

which implies that (8) exists a solution as specified in (13). This completes the proof. ∎

Corollary 1 provides a sufficient condition [i.e., (11)] making (8) feasible. Moreover, it gives a closed-form solution of problem (8) with the aid of the triangle construction. With this direct-phase selection scheme in (13), we can obtain ϕ_n, $n = 1, \ldots, N$, according to (9) and then realize the one-point phase-only array response adjustment as stated in Section II-A.

To give a validation of the above result, let us consider a ULA of $N = 16$ isotropic elements with half-wavelength space. We fix the beam axis at $\theta_0 = -20°$ and take $\mathbf{w}_{\mathrm{pre}} = \mathbf{a}(\theta_0)$. Meanwhile, we set $\theta_c = 30°$, $\rho_c = -40$ dB, and $\psi_c = 0$. In this case, we can figure out that $m = 8$, $d_1 = 1.0099$, $Q(2, m) = 7.0412$, $Q(m + 1, N) = 7.9451$, $\alpha_1 = 151.7380°$, and $\alpha_2 = 3.4504°$. Fig. 3 depicts the beampattern of $\mathbf{w}_{\mathrm{pre}}$ and the counterpart of $\mathbf{w}_{\mathrm{new}}$ using the

[1] In this work, the triangle includes the degraded case when three edges are colinear. In the degraded scenario, we have $d_1 = Q(2, m) + Q(m + 1, N)$, $\alpha_1 = 0$, and $\alpha_2 = \pi$.

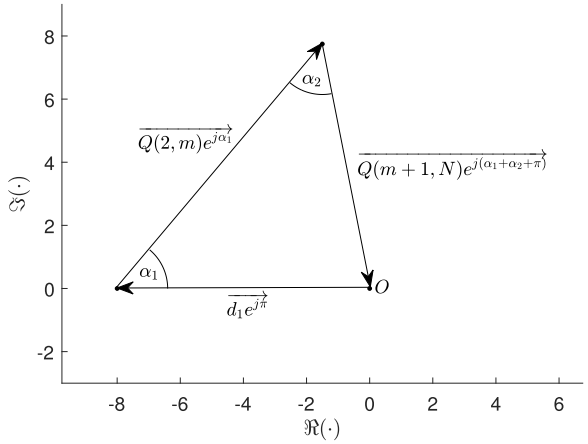

Fig. 2. Geometric illustration of triangle construction.

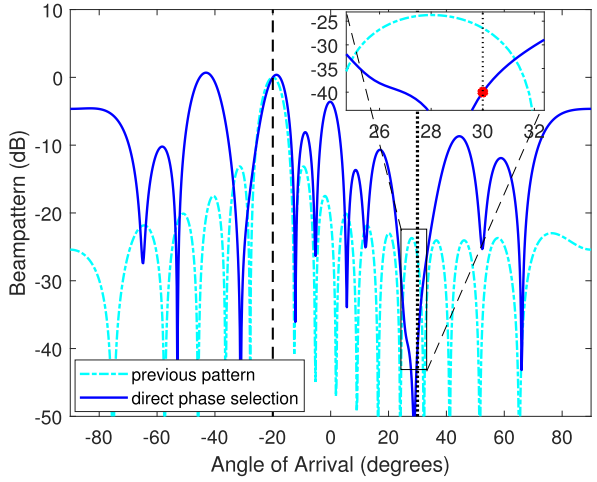

Fig. 3. Result of phase-only control via triangle construction.

direct-phase selection scheme in (13). One can see that the array power response at θ_c has been precisely adjusted as ρ_c. Moreover, it can be checked that the resulting $\mathbf{w}_{\text{new}}$ has the same element moduli as those of $\mathbf{w}_{\text{pre}}$. However, it is observed from Fig. 3 that the resulting beampattern of $\mathbf{w}_{\text{new}}$ has large pattern variations at the uncontrolled region (compared to the previous beampattern), and a serious pattern distortion is resulted. In the sequel, remedies are proposed to avoid the pattern distortion.

C. Solution Analysis via Polygon Construction

In this section, the above-obtained solution is analyzed with the polygon construction. Moreover, the range of feasible φ_n in (8) is specified. This lays a foundation for the ultimate solution of problem (8), and thus (6), as presented later in Section II-D. Before further discussion, we first give the following lemma, which has also been reported and proofed in [38].

Lemma 2: Given $d_1 \geq d_2 \geq \ldots \geq d_N > 0$, there exists a solution for $\sum_{i=1}^{N} \overrightarrow{d_i e^{j\varphi_i}} = \overrightarrow{\mathbf{0}}$ (or all the edges d_i's can form a polygon), if and only if the condition $d_1 \leq Q(2, N)$ is satisfied.

Stronger than the sufficient condition given in Corollary 1 in Section II-B, it is shown in Lemma 2 that $d_1 \leq Q(2, N)$ is also a necessary result when the problem $\sum_{i=1}^{N} \overrightarrow{d_i e^{j\varphi_i}} = \overrightarrow{\mathbf{0}}$ is feasible. With a geometric perspective, it indicates that all

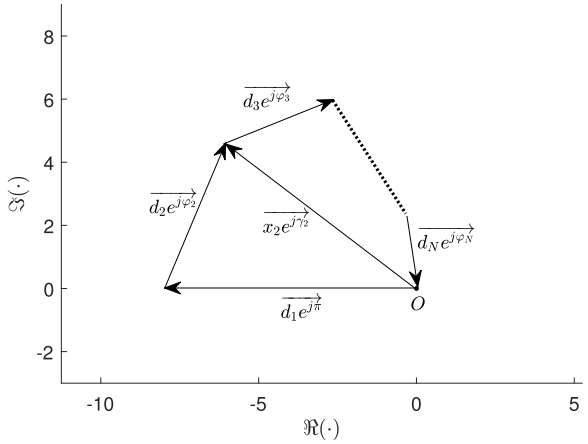

Fig. 4. Geometric illustration of polygon construction.

the edges d_i's ($i = 1, \ldots, N$) can form a polygon after the necessary rotations, if and only if the largest edge (i.e., d_1) is not greater than the summation of the remaining ones. Interestingly, if $N = 3$ applies, Lemma 2 shows that the edges d_1, d_2, and d_3 can form a triangle (the unique type of polygon in this specific case) if and only if $d_1 \leq d_2 + d_3$. This is actually a common sense for triangle construction (note that $d_1 \geq d_2 - d_3$ has been satisfied in this scenario due to the fact that $d_1 \geq d_2 \geq d_3 > 0$). With the above important observations, one can analyze the solution of $\sum_{i=1}^{N} \overrightarrow{d_i e^{j\varphi_i}} = \overrightarrow{\mathbf{0}}$ as below.

Because the identity $\sum_{i=1}^{N} \overrightarrow{d_i e^{j\varphi_i}} = \overrightarrow{\mathbf{0}}$ holds true for any phase shift, following Fig. 2, we select φ_1 for convenience as

$$\varphi_{1,\star} = \pi. \tag{19}$$

According to Corollary 1, we can form a triangle using d_1, $Q(2, m)$, and $Q(m + 1, N)$, as shown in Fig. 2, with m being given in (14). In fact, a polygon can be retained if we rotate the vector $\overrightarrow{d_2 e^{j\varphi_2}}$ with certain angles. To see it clearly, let us draw an auxiliary vector $\overrightarrow{x_2 e^{j\gamma_2}}$ (with modulus x_2 and phase γ_2) pointing from $\overrightarrow{\mathbf{0}}$ to $\overrightarrow{d_1 e^{j\pi}} + \overrightarrow{d_2 e^{j\varphi_2}}$, as depicted in Fig. 4. It can be observed that all the edges d_i's ($i = 1, \ldots, N$) can form a polygon if and only if

1) The edges d_1, d_2 and x_2 can form a triangle.
2) The edges x_2, d_3, ..., d_N can form a polygon.

Recalling Lemma 2, the above two conditions are satisfied if and only if

$$d_1 - d_2 \leq x_2 \leq d_1 + d_2 \tag{20a}$$

$$d_3 \geq x_2, \; d_3 \leq x_2 + \sum_{k=4}^{N} d_k \tag{20b}$$

or

$$d_1 - d_2 \leq x_2 \leq d_1 + d_2 \tag{21a}$$

$$x_2 \geq d_3, \; x_2 \leq \sum_{k=3}^{N} d_k. \tag{21b}$$

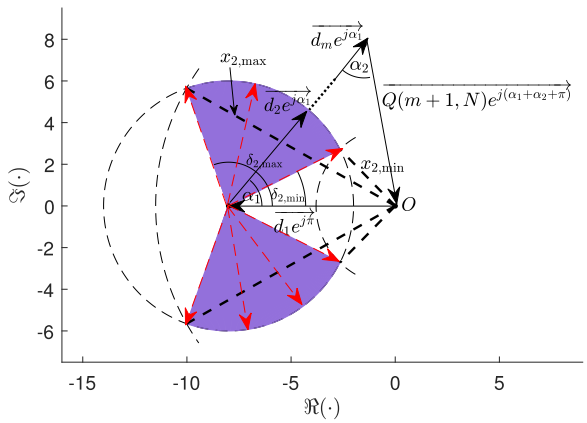

Fig. 5. Geometric illustration on the determination of the range of φ_2.

After some manipulations, one can further obtain the range of x_2 (denoted by $\mathbb{X}_2 = [x_{2,\min}, x_{2,\max}]$) as

$$x_2 \in \Bigg[\underbrace{\max\left\{d_1 - d_2, d_3 - \sum_{k=4}^{N} d_k\right\}}_{\triangleq x_{2,\min}}, \underbrace{\min\left\{d_1 + d_2, \sum_{k=3}^{N} d_k\right\}}_{\triangleq x_{2,\max}}\Bigg] \triangleq \mathbb{X}_2. \tag{22}$$

With the auxiliary vector $\overrightarrow{x_2 e^{j\gamma_2}}$ and the range of x_2 in (22), we can further determine the set of feasible φ_2. More specifically, since the edges d_1, d_2, and x_2 can form a triangle, the included angle between edges d_1 and d_2 (denote as δ_2) can be expressed as

$$\delta_2 = \operatorname{acos}\left(\frac{d_1^2 + d_2^2 - x_2^2}{2d_1 d_2}\right). \tag{23}$$

Recalling that x_2 can be varied in the set $\mathbb{X}_2$, we can readily obtain that

$$\delta_2 \in [\delta_{2,\min}, \delta_{2,\max}] \tag{24}$$

where

$$\delta_{2,\min} = \operatorname{acos}\left(\frac{d_1^2 + d_2^2 - x_{2,\min}^2}{2d_1 d_2}\right) \tag{25a}$$

$$\delta_{2,\max} = \operatorname{acos}\left(\frac{d_1^2 + d_2^2 - x_{2,\max}^2}{2d_1 d_2}\right). \tag{25b}$$

Note that the edge d_2 can be rotated clockwise or counterclockwise (by an angle δ_2) along the direction of $-\overrightarrow{d_1 e^{j\pi}}$. Then, the range of φ_2 is given by

$$\varphi_2 \in [-\delta_{\max}, -\delta_{\min}] \cup [\delta_{\min}, \delta_{\max}]. \tag{26}$$

To give a better understanding of the above descriptions, we depict Fig. 5 to present more details. The feasible $\overrightarrow{d_2 e^{j\varphi_2}}$'s are depicted in Fig. 5 as red dashed arrows, and the purple zone is their swept area. Once φ_2 is determined as $\varphi_{2,\star}$ (see more specifically in Section II-D), the resulting $\overrightarrow{x_2 e^{j\gamma_{2,\star}}}$ ($\gamma_{2,\star}$ represents the ultimate selection of γ_2) satisfies

$$\overrightarrow{x_2 e^{j\gamma_{2,\star}}} = \overrightarrow{d_1 e^{j\varphi_{1,\star}}} + \overrightarrow{d_2 e^{j\varphi_{2,\star}}}. \tag{27}$$

For the given $\overrightarrow{d_1 e^{j\varphi_{1,\star}}}$, $\overrightarrow{d_2 e^{j\varphi_{2,\star}}}$ and the resultant $\overrightarrow{x_2 e^{j\gamma_{2,\star}}}$, we can further obtain the set of feasible φ_3 with the similar manner. To satisfy (8), the edges $x_2, d_3, \ldots, d_N$ should form a polygon. In this case, one can draw an auxiliary vector $\overrightarrow{x_3 e^{j\gamma_3}}$ pointing from $\overrightarrow{\mathbf{0}}$ to $\overrightarrow{x_2 e^{j\gamma_{2,\star}}} + \overrightarrow{d_3 e^{j\varphi_3}}$. Then, the edges x_2, $d_3, \ldots, d_N$ can form a polygon if and only if

1) The edges x_2, d_3, and x_3 can form a triangle.
2) The edges x_3, d_4, …, d_N can form a polygon.

Following the determination procedure of the set of feasible φ_2, we can then obtain the set of φ_3 accordingly. On this basis, the ultimate selection of φ_3 can be determined according to some criteria (see Section II-D), and the resulting $\overrightarrow{x_3 e^{j\gamma_{3,\star}}}$ satisfies

$$\overrightarrow{x_3 e^{j\gamma_{3,\star}}} = \overrightarrow{x_2 e^{j\gamma_{2,\star}}} + \overrightarrow{d_3 e^{j\varphi_{3,\star}}} = \sum_{k=1}^{3} \overrightarrow{d_k e^{j\varphi_{k,\star}}}. \tag{28}$$

In a general sense, if $\overrightarrow{x_{i-1} e^{j\gamma_{i-1}}}$ has been determined as $\overrightarrow{x_{i-1} e^{j\gamma_{i-1,\star}}}$ satisfying

$$\overrightarrow{x_{i-1} e^{j\gamma_{i-1,\star}}} = \overrightarrow{x_{i-2} e^{j\gamma_{i-2,\star}}} + \overrightarrow{d_{i-1} e^{j\varphi_{i-1,\star}}} = \sum_{k=1}^{i-1} \overrightarrow{d_k e^{j\varphi_{k,\star}}} \tag{29}$$

we can then calculate the feasible set of φ_i, by drawing an auxiliary vector $\overrightarrow{x_i e^{j\gamma_i}}$ pointing from $\overrightarrow{\mathbf{0}}$ to $\overrightarrow{x_{i-1} e^{j\gamma_{i-1,\star}}} + \overrightarrow{d_i e^{j\varphi_i}}$, $i = 2, \ldots, N-2$, where x_1 and $\gamma_{1,\star}$ are defined, respectively, as

$$x_1 \triangleq d_1 \tag{30a}$$

$$\gamma_{1,\star} \triangleq \varphi_{1,\star} = \pi. \tag{30b}$$

To satisfy (8), the edges x_{i-1}, $d_i, \ldots, d_N$ should form a polygon. With similar manipulations, we can obtain the set of x_i (denoted as $\mathbb{X}_i$) as

$$x_i \in \Bigg[\underbrace{\max\left\{\left|x_{i-1} - d_i\right|, d_{i+1} - \sum_{k=i+2}^{N} d_k\right\}}_{\triangleq x_{i,\min}}, \underbrace{\min\left\{x_{i-1} + d_i, \sum_{k=i+1}^{N} d_k\right\}}_{\triangleq x_{i,\max}}\Bigg] \triangleq \mathbb{X}_i, \quad 2 \le i \le N-2 \tag{31}$$

where i can be taken as $2, \ldots, N-2$. Before further studying the feasible set of φ_i, we first derive the following proposition that guarantees the nonnullity of the set $\mathbb{X}_i$, $i = 2, \ldots, N-2$.

Proposition 1: The set $\mathbb{X}_2$ is nonempty if $d_1 \le Q(2, N)$. For $i = 3, \ldots, N-2$, $\mathbb{X}_i$ is nonempty if $x_{i-1} \in \mathbb{X}_{i-1}$.

Proof: See Appendix A. ∎

Since each x_{i-1} is selected from the corresponding set $\mathbb{X}_{i-1}$ ($i = 3, \ldots, N-2$), one can learn from Proposition 1 that all the set $\mathbb{X}_i$'s ($i = 2, \ldots, N-2$) are nonempty, provided that $d_1 \le Q(2, N)$ is satisfied. On this basis, Fig. 6 presents

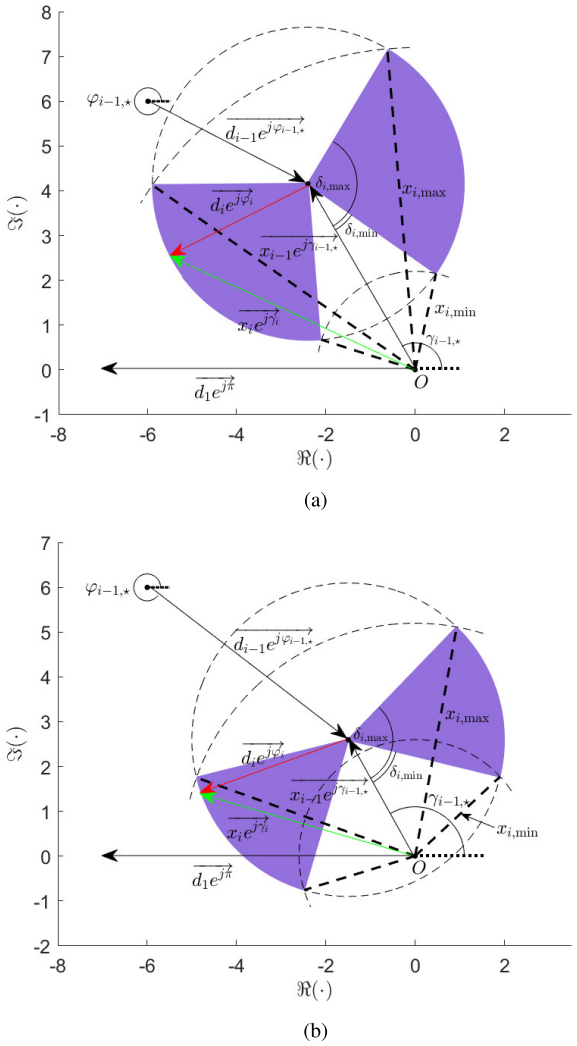

Fig. 6. Geometric illustration on the determination of the set of a generalized φ_i, $i = 2, \ldots, N-2$. (a) $x_{i-1} \geq d_i$. (b) $x_{i-1} < d_i$.

a geometric interpretation on how to determine the set of a generalized φ_i ($i = 2, \ldots, N-2$). To have a comprehensive description, two cases, i.e., $x_{i-1} \geq d_i$ and $x_{i-1} < d_i$, are considered in Fig. 6(a) and (b), respectively. As illustrated, the included angle between edges x_{i-1} and d_i (denoted as δ_i) can be expressed in both scenarios as

$$\delta_i = \operatorname{acos}\left(\frac{x_{i-1}^2 + d_i^2 - x_i^2}{2x_{i-1}d_i}\right), \quad i = 2, \ldots, N-2. \tag{32}$$

Combining (31), one can readily find that

$$\delta_i \in [\delta_{i,\min},\ \delta_{i,\max}] \tag{33}$$

with

$$\delta_{i,\min} = \operatorname{acos}\left(\frac{x_{i-1}^2 + d_i^2 - x_{i,\min}^2}{2x_{i-1}d_i}\right) \tag{34a}$$

$$\delta_{i,\max} = \operatorname{acos}\left(\frac{x_{i-1}^2 + d_i^2 - x_{i,\max}^2}{2x_{i-1}d_i}\right) \tag{34b}$$

where both $x_{i,\min}$ and $x_{i,\max}$ are defined as in (31), $i = 2, \ldots, N-2$. Furthermore, we can obtain the set of

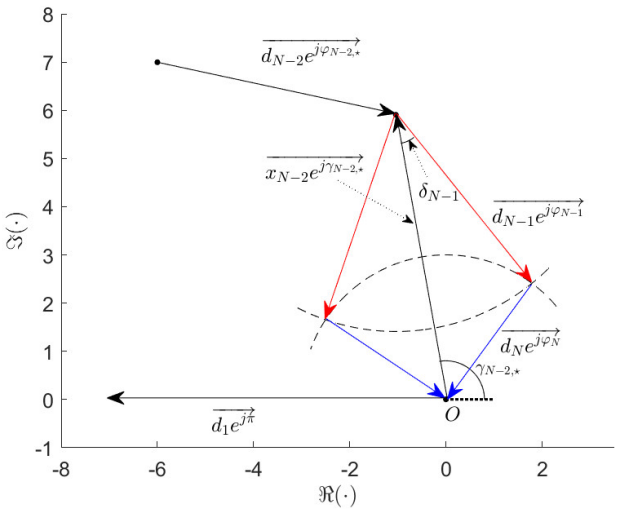

Fig. 7. Geometric illustration on the candidates of φ_{N-1} and φ_N.

feasible φ_i, $i = 2, \ldots, N-2$, as

$$\varphi_i \in \Psi_i \triangleq [\gamma_{i-1,\star} + \pi - \delta_{i,\max}, \gamma_{i-1,\star} + \pi - \delta_{i,\min}] \cup [\gamma_{i-1,\star} + \pi + \delta_{i,\min}, \gamma_{i-1,\star} + \pi + \delta_{i,\max}]. \tag{35}$$

The purple zone in Fig. 6 is the resulting swept area of $\overrightarrow{d_i e^{j\varphi_i}}$, and the red arrow gives an illustration for $\overrightarrow{d_i e^{j\varphi_i}}$. Interestingly, it is not hard to find that we have $\delta_{i,\min} = 0$ and $\delta_{i,\max} = \pi$, provided that

$$\left|x_{i-1} - d_i\right| \geq d_{i+1} - \sum_{k=i+2}^{N} d_k \tag{36a}$$

$$x_{i-1} + d_i \leq \sum_{k=i+1}^{N} d_k. \tag{36b}$$

In this case, the range of φ_i (i.e., Ψ_i) becomes $[0, 2\pi]$.

Once φ_i has been determined as $\varphi_{i,\star}$ (according to some criteria discussed later), the ultimate $\overrightarrow{x_i e^{j\gamma_{i,\star}}}$, $i = 2, \ldots, N-2$, can be generally expressed as

$$\overrightarrow{x_i e^{j\gamma_{i,\star}}} = \overrightarrow{x_{i-1} e^{j\gamma_{i-1,\star}}} + \overrightarrow{d_i e^{j\varphi_{i,\star}}}. \tag{37}$$

In the above discussions, the sets of φ_is are specified for $i < N-2$. Note that if $i = N-2$ applies, the resulting x_{N-2} can form a triangle (the unique type of polygon for three edges) with the other two edges d_{N-1} and d_N, as presented in Fig. 7. It is not hard to specify the ranges of the remaining two phases, i.e., φ_{N-1} and φ_N. More specifically, to find the qualified candidates of φ_{N-1}, we can first express the included angle between edges x_{N-2} and d_{N-1} as

$$\delta_{N-1} = \operatorname{acos}\left(\frac{x_{N-2}^2 + d_{N-1}^2 - d_N^2}{2x_{N-2}d_{N-1}}\right). \tag{38}$$

With the geometric interpretation in Fig. 7, one can learn that there are two candidates at most for φ_{N-1} as

$$\varphi_{N-1} \in \Psi_{N-1} \triangleq \{\gamma_{N-2,\star} + \pi - \delta_{N-1}, \gamma_{N-2,\star} + \pi + \delta_{N-1}\}. \tag{39}$$

Moreover, it can be readily obtained from Fig. 7 that

$$\overrightarrow{d_N e^{j\varphi_N}} = -(\overrightarrow{x_{N-2}e^{j\gamma_{N-2,\star}}} + \overrightarrow{d_{N-1}e^{j\varphi_{N-1}}}). \tag{40}$$

If φ_{N-1} is selected as $\varphi_{N-1,\star}$ (discussed later in Section II-D), there will be one choice for the ultimate φ_N (denoted as $\varphi_{N,\star}$), which can be expressed accordingly as

$$\varphi_{N,\star} = \angle(\overrightarrow{x_{N-2}e^{j\gamma_{N-2,\star}}} + \overrightarrow{d_{N-1}e^{j\varphi_{N-1,\star}}}) + \pi. \tag{41}$$

D. Phase Determination

In Section II-C, a detailed analysis on the solution of (8) has been given and the set of feasible φ_i $(i = 2, \ldots, N)$ has been specified one-by-one. In this section, we consider the determination of $\varphi_{i,\star}$, $i = 2, \ldots, N$ and complete the proposed algorithm by finding the ultimate ϕ_n, $n = 1, \ldots, N$.

To begin with, we can first obtain from (9) that

$$\mathbf{J}[\phi_1, \ldots, \phi_N]^{\mathrm{T}} = \mathbf{J}[\vartheta_1, \ldots, \vartheta_N]^{\mathrm{T}} - [\varphi_1, \ldots, \varphi_N]^{\mathrm{T}}. \tag{42}$$

Then, for any given $i \in \{1, \ldots, N\}$, there exists a unique index $n \in \{1, \ldots, N\}$ such that $\mathbf{J}(i, n) = 1$, and we denote its resulting value for clarity as

$$n = \varsigma(i) \tag{43}$$

where $\varsigma(\cdot)$ returns an index from 1 to N, and the specific formulation of $\varsigma(\cdot)$ depends on the permutation matrix $\mathbf{J}$. With the above notation, it can be obtained from (42) that

$$\phi_{\varsigma(i)} = \vartheta_{\varsigma(i)} - \varphi_i, \quad i = 1, \ldots, N. \tag{44}$$

Since the beampattern is invariant to a fixed phase shift and $\varphi_{1,\star} = \pi$ is taken, we set the ultimate selection of $\phi_{\varsigma(1)}$ as

$$\phi_{\varsigma(1),\star} = \vartheta_{\varsigma(1)} - \varphi_{1,\star} = \vartheta_{\varsigma(1)} - \pi. \tag{45}$$

For $i \in \{2, \ldots, N-1\}$, we can determine φ_i indirectly according to the selection of $\phi_{\varsigma(i)}$. More specifically, suppose that the set of φ_i is known (see Section II-C for the specification of the set). Since $\vartheta_{\varsigma(i)}$ is a constant, one can readily derive [according to (44)] the set of $\phi_{\varsigma(i)}$ (denoted by $\Phi_{\varsigma(i)}$) as

$$\Phi_{\varsigma(i)} = \{\phi_{\varsigma(i)} | \phi_{\varsigma(i)} = (\vartheta_{\varsigma(i)} - \varphi_i)_{2\pi},\ \varphi_i \in \Psi_i\} \tag{46}$$

which can be expressed more precisely as

$$\Phi_{\varsigma(i)} = \begin{cases} \left(\left[a^{(l)}_{\varsigma(i)}, a^{(r)}_{\varsigma(i)}\right] \right. \\ \quad \left. \cup \left[b^{(l)}_{\varsigma(i)}, b^{(r)}_{\varsigma(i)}\right]\right)_{2\pi}, & \text{if } i \in \{2, \ldots, N-2\} \\ \left(\left\{c^{(l)}_{\varsigma(N-1)}, c^{(r)}_{\varsigma(N-1)}\right\}\right)_{2\pi}, & \text{if } i = N-1 \end{cases} \tag{47}$$

where

$$a^{(l)}_{\varsigma(i)} \triangleq \vartheta_{\varsigma(i)} - \gamma_{i-1,\star} - \pi - \delta_{i,\max} \tag{48a}$$

$$a^{(r)}_{\varsigma(i)} \triangleq \vartheta_{\varsigma(i)} - \gamma_{i-1,\star} - \pi - \delta_{i,\min} \tag{48b}$$

$$b^{(l)}_{\varsigma(i)} \triangleq \vartheta_{\varsigma(i)} - \gamma_{i-1,\star} - \pi + \delta_{i,\min} \tag{48c}$$

$$b^{(r)}_{\varsigma(i)} \triangleq \vartheta_{\varsigma(i)} - \gamma_{i-1,\star} - \pi + \delta_{i,\max} \tag{48d}$$

for $i \in \{2, \ldots, N-2\}$, and

$$c^{(l)}_{\varsigma(N-1)} \triangleq \vartheta_{\varsigma(N-1)} - \gamma_{N-2,\star} - \pi - \delta_{N-1} \tag{49a}$$

$$c^{(r)}_{\varsigma(N-1)} \triangleq \vartheta_{\varsigma(N-1)} - \gamma_{N-2,\star} - \pi + \delta_{N-1}. \tag{49b}$$

To avoid large pattern variations in the uncontrolled region, we propose to choose $\phi_{\varsigma(i)}$ $(i = 1, \ldots, N)$ as close as possible to the corresponding phase of a predesigned weight with desirable beampattern. More specifically, we optimize $\phi_{\varsigma(i)}$ $(i = 2, \ldots, N-1)$ as

$$\min_{\phi_{\varsigma(i)}} \ |\exp(j\phi_{\varsigma(i)}) - \exp(j\angle\overline{w}_{\varsigma(i)})| \tag{50a}$$

$$\text{s. t. } \phi_{\varsigma(i)} \in \Phi_{\varsigma(i)}. \tag{50b}$$

In (50), $\overline{w}_{\varsigma(i)}$ is the $\varsigma(i)$th element of a predesigned weight vector $\overline{\mathbf{w}}$ that can result a satisfactory beampattern, e.g., desired response level at θ_c and/or small pattern variations at the uncontrolled region. Note that $\overline{\mathbf{w}}$ may not satisfy the phase-only constraint. Thus, $\overline{\mathbf{w}}$ is imperfect with some desirable characteristics. In addition, $\overline{\mathbf{w}}$ is predesigned to satisfy

$$\angle\overline{w}_{\varsigma(1)} = \vartheta_{\varsigma(1)} - \pi. \tag{51}$$

As a result, we already have $\phi_{\varsigma(1),\star} = \angle\overline{w}_{\varsigma(1)}$, which is the optimal solution of (50) when $i = 1$ applies. For $i \in \{2, \ldots, N-1\}$, it is not difficult to derive that the problem (50) has the following analytical solution:

$$\phi_{\varsigma(i),\star} = \begin{cases} \angle\overline{w}_{\varsigma(i)}, & \text{if } (\angle\overline{w}_{\varsigma(i)})_{2\pi} \in \Phi_{\varsigma(i)} \\ \tau_{\varsigma(i)}, & \text{otherwise} \end{cases} \tag{52}$$

where $\tau_{\varsigma(i)}$ is the optimal solution of the problem

$$\max_{\tau} \ \cos(\tau - \angle\overline{w}_{\varsigma(i)}) \tag{53a}$$

$$\text{s.t. } \tau \in \begin{cases} \left\{a^{(l)}_{\varsigma(i)}, a^{(r)}_{\varsigma(i)}, b^{(l)}_{\varsigma(i)}, b^{(r)}_{\varsigma(i)}\right\}, & \text{if } i \in \{2, \ldots, N-2\} \\ \left\{c^{(l)}_{\varsigma(N-1)}, c^{(r)}_{\varsigma(N-1)}\right\}, & \text{if } i = N-1 \end{cases} \tag{53b}$$

which can be solved by simple comparison operations.

In the above formulating problem (50), the phase $\phi_{\varsigma(i)}$ is actually designed to be the closest one to the phase of $\overline{w}_{\varsigma(i)}$. In such a manner, the resulting pattern may perform similar to that of the weight vector $\overline{\mathbf{w}}$. Thus, it is very likely to result small pattern variations at the uncontrolled region.

In this paper, we propose to construct $\overline{\mathbf{w}}$ using the weight vector orthogonal decomposition (WORD) algorithm [9]. Giving the weight vector $\mathbf{w}_{\mathrm{pre}}$, the WORD algorithm is able to precisely adjust array response level at one preassigned angle θ_c as the desired level ρ_c, with a closed-form solution. More specifically, the new weight vector satisfying the single-point response requirement is analytically expressed as

$$\breve{\mathbf{w}} = \left[\mathbf{w}_{\perp} \quad \mathbf{w}_{\parallel}\right]\left[1 \ \beta\right]^{\mathrm{T}} \tag{54}$$

where $\mathbf{w}_{\perp}$ and $\mathbf{w}_{\parallel}$ are orthogonally decomposed from the previous weight vector $\mathbf{w}_{\mathrm{pre}}$ as

$$\mathbf{w}_{\perp} \triangleq \mathbf{P}^{\perp}_{\mathbf{a}(\theta_c)}\mathbf{w}_{\mathrm{pre}}, \quad \mathbf{w}_{\parallel} \triangleq \mathbf{P}_{\mathbf{a}(\theta_c)}\mathbf{w}_{\mathrm{pre}}. \tag{55}$$

In (54), the real-valued number β can be selected to be either β_a or β_b, both of which can be determined by the desired level ρ_c at θ_c. In [9], it has been derived that

$$\beta_a = \frac{-\Re(\mathbf{B}(1,2)) + \eta}{\mathbf{B}(2,2)}, \quad \beta_b = \frac{-\Re(\mathbf{B}(1,2)) - \eta}{\mathbf{B}(2,2)} \tag{56}$$

where $\mathbf{B}$ and η satisfy

$$\mathbf{B} = \begin{bmatrix} \mathbf{w}_\perp^{\mathrm{H}}\mathbf{a}(\theta_c) \\ \mathbf{w}_\parallel^{\mathrm{H}}\mathbf{a}(\theta_c) \end{bmatrix}\begin{bmatrix} \mathbf{w}_\perp^{\mathrm{H}}\mathbf{a}(\theta_c) \\ \mathbf{w}_\parallel^{\mathrm{H}}\mathbf{a}(\theta_c) \end{bmatrix}^{\mathrm{H}} - \rho_c \begin{bmatrix} \mathbf{w}_\perp^{\mathrm{H}}\mathbf{a}(\theta_0) \\ \mathbf{w}_\parallel^{\mathrm{H}}\mathbf{a}(\theta_0) \end{bmatrix}\begin{bmatrix} \mathbf{w}_\perp^{\mathrm{H}}\mathbf{a}(\theta_0) \\ \mathbf{w}_\parallel^{\mathrm{H}}\mathbf{a}(\theta_0) \end{bmatrix}^{\mathrm{H}} \tag{57}$$

$$\eta = \sqrt{\Re^2(\mathbf{B}(1,2)) - \mathbf{B}(1,1)\mathbf{B}(2,2)}. \tag{58}$$

To obtain the ultimate expression of $\breve{\mathbf{w}}$ that adjusts the response level of θ_c to ρ_c, the one (either β_a or β_b) that minimizes $F(\beta) = \|\mathbf{P}_{\mathbf{w}_{\mathrm{pre}}}^{\perp}\breve{\mathbf{w}}/\|\breve{\mathbf{w}}\|_2\|_2^2$ is selected. To satisfy (51), we carry out a phase shifting to $\breve{\mathbf{w}}$ and obtain the ultimate $\overline{\mathbf{w}}$ as

$$\overline{\mathbf{w}} = \breve{\mathbf{w}} \cdot \exp\left(j\left(\vartheta_{\varsigma(1)} - \pi - \angle\breve{w}_{\varsigma(1)}\right)\right) \tag{59}$$

where $\breve{w}_{\varsigma(1)}$ is the $\varsigma(1)$th element of the weight vector $\breve{\mathbf{w}}$. Note that both $\breve{\mathbf{w}}$ and $\overline{\mathbf{w}}$ may not satisfy the phase-only constraint.

Once the problem (50) has been solved with the aid of the predesigned $\overline{\mathbf{w}}$ in (59), the ultimate $\varphi_{i,\star}$ can be expressed according to (44) as

$$\varphi_{i,\star} = \vartheta_{\varsigma(i)} - \phi_{\varsigma(i),\star}, \ i = 2, \ldots, N-1 \tag{60}$$

which is necessary for the selections of the follow-up phases, i.e., $\varphi_{i+1}, \ldots, \varphi_N$. In addition, it should be pointed out that the setting of $\overline{\mathbf{w}}$ is flexible and may have other choices different from (59). Extensive simulations show that the selection of $\overline{\mathbf{w}}$ in (59) obtains desirable results under various situations.

When $i = N$ applies, there is only one candidate for φ_N, whose ultimate value can be obtained according to (41). Thus, one can calculate the corresponding $\phi_{\varsigma(N),\star}$ as

$$\phi_{\varsigma(N),\star} = \vartheta_{\varsigma(N)} - \varphi_{N,\star}. \tag{61}$$

This completes the determination of $\phi_{\varsigma(i),\star}$, $i = 1, \ldots, N$. On this basis, one can express the new weight vector $\mathbf{w}_{\mathrm{new}}$ as

$$\mathbf{w}_{\mathrm{new}} = [|w_{\mathrm{pre},1}|, \ldots, |w_{\mathrm{pre},N}|]^{\mathrm{T}} \odot [e^{j\phi_{1,\star}}, \ldots, e^{j\phi_{N,\star}}]^{\mathrm{T}}. \tag{62}$$

In addition, extensive simulations show that an outstanding performance can be resulted if the ψ_c in (4) is taken as

$$\psi_c = \angle\left(\overline{\mathbf{w}}^{\mathrm{H}}\mathbf{a}(\theta_c)/\overline{\mathbf{w}}^{\mathrm{H}}\mathbf{a}(\theta_0)\right). \tag{63}$$

With this setting, the resulting phase of the normalized array response [i.e., $\overline{\mathbf{w}}^{\mathrm{H}}\mathbf{a}(\theta)/\overline{\mathbf{w}}^{\mathrm{H}}\mathbf{a}(\theta_0)$] would be unaltered at the direction θ_c, compared to that of $\overline{\mathbf{w}}$ or $\breve{\mathbf{w}}$. This completes the descriptions of the proposed fast array response adjustment algorithm with phase-only constraint. To make it clear, we summarize our algorithm in Algorithm 1 and present its corresponding flowchart in Fig. 8.

To validate the performance of the proposed algorithm, we follow the test in Section II-B and consider a ULA of $N = 16$ isotropic elements with half-wavelength space. The same as the previous setting, we take $\theta_0 = -20°$, $\theta_c = 30°$, $\rho_c = -40$ dB, and $\mathbf{w}_{\mathrm{pre}} = \mathbf{a}(\theta_0)$. In this case, the moduli of $\mathbf{w}_{\mathrm{pre}}$ are all ones, i.e., $|w_{\mathrm{pre},n}| = 1$, $n = 1, \ldots, N$. Following the descriptions in Algorithm 1, we can figure out

Algorithm 1 Proposed Fast Array Response Adjustment Algorithm

give θ_0, θ_c, ρ_c and the previous weight vector $\mathbf{w}_{\mathrm{pre}}$
calculate β_a and β_b in (56), and obtain the resulting weight vector $\breve{\mathbf{w}}$ in (54)
obtain $\psi_c = \angle(\overline{\mathbf{w}}^{\mathrm{H}}\mathbf{a}(\theta_c)/\overline{\mathbf{w}}^{\mathrm{H}}\mathbf{a}(\theta_0))$
obtain $\mathbf{h}(\theta_c, \theta_0, \rho_c, \psi_c) = \mathbf{a}(\theta_c) - \sqrt{\rho_c}e^{j\psi_c}\mathbf{a}(\theta_0)$
denote $\upsilon_n = h_n \cdot |w_{\mathrm{pre},n}|$, $n = 1, \ldots, N$
reorder $|\upsilon_1|, \ldots, |\upsilon_N|$, and obtain $[d_1, \ldots, d_N]^{\mathrm{T}} = \mathbf{J}[|\upsilon_1|, \ldots, |\upsilon_N|]^{\mathrm{T}}$
obtain $\overline{\mathbf{w}} = \breve{\mathbf{w}} \cdot \exp(j(\vartheta_{\varsigma(1)} - \pi - \angle\breve{w}_{\varsigma(1)}))$
for $i = 1, 2, \ldots, N-1$ **do**
  if $i == 1$ **then**
    set $\varphi_{1,\star} = \gamma_{1,\star} = \pi$, $\phi_{\varsigma(1),\star} = \vartheta_{\varsigma(1)} - \pi$, $x_1 = d_1$
  else if $i \in \{2, \ldots, N-2\}$ **then**
    obtain $x_{i,\min}$ and $x_{i,\max}$ in (31), and calculate $\delta_{i,\min}$ and $\delta_{i,\max}$ in (34), respectively
    obtain the set $\Phi_{\varsigma(i)}$ in (47) and find the optimal solution $\phi_{\varsigma(i),\star}$ in (52) for the problem (50)
    obtain $\varphi_{i,\star} = \vartheta_{\varsigma(i)} - \phi_{\varsigma(i),\star}$
    obtain $\overrightarrow{x_i e^{j\gamma_{i,\star}}} = \overrightarrow{x_{i-1}e^{j\gamma_{i-1,\star}}} + \overrightarrow{d_i e^{j\varphi_{i,\star}}}$
  else
    calculate δ_{N-1} in (38)
    obtain the set $\Phi_{\varsigma(N-1)}$ in (47) and find the optimal solution $\phi_{\varsigma(N-1),\star}$ in (52) for the problem (50)
    obtain $\varphi_{N-1,\star} = \vartheta_{\varsigma(N-1)} - \phi_{\varsigma(N-1),\star}$
    take
$$\varphi_{N,\star} = \angle(\overrightarrow{x_{N-2}e^{j\gamma_{N-2,\star}}} + \overrightarrow{d_{N-1}e^{j\varphi_{N-1,\star}}}) + \pi$$
    obtain $\phi_{\varsigma(N),\star} = \vartheta_{\varsigma(N)} - \varphi_{N,\star}$
  end if
end for
construct the entries of the new weight vector by $w_{\mathrm{new},\varsigma(i)} = |w_{\mathrm{pre},\varsigma(i)}| \cdot e^{j\phi_{\varsigma(i),\star}}$, $i = 1, \ldots, N$, and then output the resulting $\mathbf{w}_{\mathrm{new}}$ and the corresponding beampattern $L_{\mathrm{new}}(\theta, \theta_0)$

TABLE I
RESULTING VALUES OF $\breve{\mathbf{w}}$ AND $\angle\overline{\mathbf{w}}$

n	$\breve{w}_n$	$\angle\overline{w}_n$	n	$\breve{w}_n$	$\angle\overline{w}_n$
1	$0.9799e^{+j0.0320}$	1.1808	9	$0.9914e^{-j2.3494}$	−1.2007
2	$1.0039e^{-j1.1118}$	0.0370	10	$1.0258e^{+j2.9229}$	−2.2116
3	$1.0156e^{-j2.1151}$	−0.9664	11	$0.9646e^{+j1.8089}$	2.9576
4	$0.9707e^{+j3.0359}$	−2.0985	12	$1.0370e^{+j0.7410}$	1.8897
5	$1.0370e^{+j1.9912}$	3.1400	13	$0.9707e^{-j0.3037}$	0.8450
6	$0.9646e^{+j0.9234}$	2.0721	14	$1.0156e^{-j1.4359}$	−0.2871
7	$1.0258e^{-j0.1907}$	0.9581	15	$1.0039e^{-j2.4392}$	−1.2905
8	$0.9914e^{-j1.2015}$	−0.0528	16	$0.9799e^{+j2.7002}$	−2.4343

that $\beta_a = 0.2100$ and $\beta_b = -0.2098$. Then, the weight $\breve{\mathbf{w}}$ of WORD can be calculated (see Table I for the result), and we obtain $\psi_c = 0.9901$ according to (63). On this basis, one can obtain the phase of the entry of $\overline{\mathbf{w}}$, as also specified in Table I. According to the phase determination scheme in Algorithm 1, we can then figure out the index $\varsigma(i)$, the set

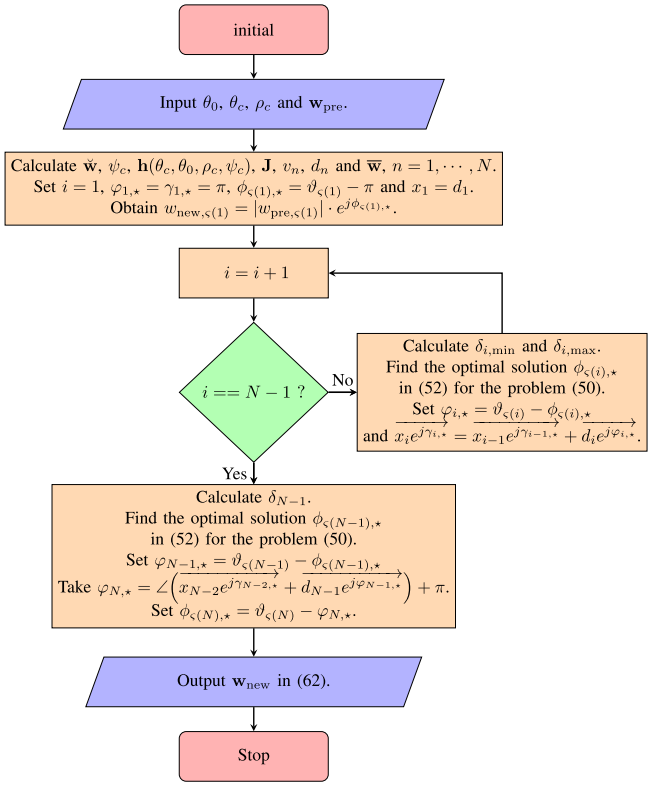

Fig. 8. Flowchart of the proposed fast array response adjustment algorithm.

TABLE II
RESULTING PARAMETERS OF THE PROPOSED ALGORITHM

i	$\varsigma(i)$	$\Phi_{\varsigma(i)}$	$\angle\overline{w}_{\varsigma(i)}$	$\phi_{\varsigma(i),\star}$
1	5	$\{3.1400\}$	3.1400	3.1400
2	12	$[-4.7107, 1.5724]$	1.8897	1.8897
3	10	$[-1.4195, 4.8637]$	-2.2116	-2.2116
4	7	$[-6.3765, -0.0934]$	0.9581	0.9581
5	3	$[-6.1337, 0.1495]$	-0.9664	-0.9664
6	14	$[-1.6332, 4.6500]$	-0.2871	-0.2871
7	15	$[-6.1345, 0.1487]$	-1.2905	-1.2905
8	2	$[-1.6229, 4.6603]$	0.0370	0.0370
9	8	$[-4.5635, 1.7197]$	-0.0528	-0.0528
10	9	$[-3.1940, 3.0891]$	-1.2007	-1.2007
11	1	$[-2.2983, 2.5988]$	1.1808	1.1808
12	16	$[-3.3042, 0.0367]$	-2.4343	-2.4343
13	13	$[-1.0997, 1.4046]$	0.8450	0.8450
14	4	$[-2.5563, -0.7786]$	-2.0985	-2.0985
15	6	$\{1.0987, 2.3536\}$	2.0721	2.3536
16	11	$\{2.6761\}$	2.9576	2.6761

$\Phi_{\varsigma(i)}$ and the value of $\phi_{\varsigma(i),\star}$ $(i=1,\ldots,N)$, see Table II for their detailed results. For simplicity, the results in Table II are not processed by the mod 2π operation. It can be checked from Table II that the range $\Phi_{\varsigma(i)}$ covers the value of $\overline{w}_{\varsigma(i)}$, and thus, $\phi_{\varsigma(i),\star}=\overline{w}_{\varsigma(i)}$ is resulted, for $i=1,\ldots,N-2$. When $i=N-1$ or $i=N$ applies, there are only two or one candidate(s) in the set $\Phi_{\varsigma(i)}$, respectively. In these two cases, the resulting $\phi_{\varsigma(N-1),\star}$ and $\phi_{\varsigma(N),\star}$ are different from the corresponding $\overline{w}_{\varsigma(N-1)}$ and $\overline{w}_{\varsigma(N)}$, respectively. In addition, note from Table I that the element moduli of $\breve{\mathbf{w}}$ (or $\overline{\mathbf{w}}$) are all close to one, which is the desired modulus of $w_{\text{new},n}$, $n=1,\ldots,N$. Thus, it can be predicted that the resulting beampattern of the proposed algorithm will be similar to the result of WORD algorithm.

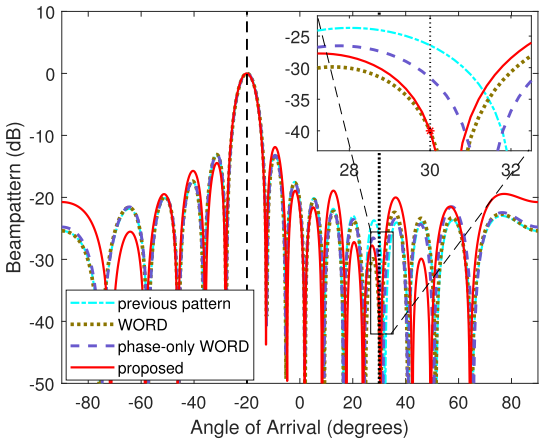

Fig. 9. Resulting patterns of different response control algorithms.

Fig. 9 compares several beampatterns of different weights in the above test. We can see that the WORD algorithm precisely adjusts the response of θ_c as desired and results in small pattern variations at the uncontrolled region. By taking the moduli to be the same as those of the previous $\mathbf{w}_{\text{pre}}$ and fixing the phases as the corresponding values of the weight $\overline{\mathbf{w}}$ in (59), we obtain a new weight and depict the corresponding beampattern in Fig. 9 labeled as with phase-only WORD. It can be observed that the obtained pattern of phase-only WORD is similar to that of the WORD algorithm, although the response at θ_c may fail to be adjusted as desired. In contrast, the proposed algorithm guarantees a precise array response adjustment at θ_c. Moreover, since the phases of our algorithm are designed to be close to those of phase-only WORD, our algorithm also brings small pattern variations at the uncontrolled region as shown in Fig. 9. This validates the superiority of the phase determination scheme in the proposed algorithm, when compared to the direct-phase selection scheme with triangle construction as presented in Section II-B.

E. Computational Complexity

It can be found that, our algorithm only requires some simple additions or comparison operators with low computational complexities. Among them, the main computation attributes to the sorting operator in (7), with a computational complexity $\mathcal{O}(N\log_2 N)$. Overall, the computational complexity of the proposed algorithm is $\mathcal{O}(N\log_2 N)$.

III. NUMERICAL RESULTS

In this section, simulations are presented to demonstrate the effectiveness of the proposed fast array response adjustment algorithm with phase-only constraint. For comparison purpose, the results of SDR method in [25] and CR method in [27] will also be presented. To test the performance of different phase-only array response adjustment algorithms, we introduce two

TABLE III
WEIGHT VECTOR COMPARISON

n	$w_{\text{pre},n}$	$\breve{w}_n$	$w_{\text{new},n}$
1	$0.2565e^{+j0.0000}$	$0.2469e^{+j0.0382}$	$0.2565e^{+j0.1926}$
2	$0.3950e^{+j1.0745}$	$0.3996e^{+j1.0423}$	$0.3950e^{+j1.0423}$
3	$0.6080e^{+j2.1490}$	$0.6101e^{+j2.1710}$	$0.6080e^{+j2.1710}$
4	$0.8069e^{-j3.0597}$	$0.7991e^{-j3.0735}$	$0.8069e^{-j3.0735}$
5	$0.9486e^{-j1.9852}$	$0.9607e^{-j1.9788}$	$0.9486e^{-j1.9788}$
6	$1.0000e^{-j0.9107}$	$0.9864e^{-j0.9107}$	$1.0000e^{-j0.9107}$
7	$0.9486e^{+j0.1637}$	$0.9607e^{+j0.1573}$	$0.9486e^{+j0.1573}$
8	$0.8069e^{+j1.2382}$	$0.7991e^{+j1.2520}$	$0.8069e^{+j1.2520}$
9	$0.6080e^{+j2.3127}$	$0.6101e^{+j2.2907}$	$0.6080e^{+j2.2907}$
10	$0.3950e^{-j2.8960}$	$0.3996e^{-j2.8638}$	$0.3950e^{-j2.8638}$
11	$0.2565e^{-j1.8215}$	$0.2469e^{-j1.8597}$	$0.2565e^{-j2.0141}$

metrics. The first one is defined as

$$D \triangleq |L_{\text{new}}(\theta_c, \theta_0) - \rho_c| \tag{64}$$

which measures the response difference between the resulting level at θ_c and the desired value ρ_c. The second metric is defined as

$$E \triangleq \sqrt{\frac{1}{N}\sum_{n=1}^{N} ||w_{\text{new},n}| - |w_{\text{pre},n}||^2} \tag{65}$$

which measures the average modulus difference between the resulting weight vector $\mathbf{w}_{\text{new}}$ and the previous $\mathbf{w}_{\text{pre}}$. Clearly, both D and E are expected to be zero for the phase-only response control, and better performance can be obtained for less D and E.

A. Phase-Only Array Response Adjustment for a ULA Starting From Chebyshev Weight

In the first example, a linearly half-wavelength spaced array with 11 isotropic elements is considered. We take the main beam axis as $\theta_0 = 20°$ and prescribe the controlled angle as $\theta_c = -54°$ and its desired level as $\rho_c = -45$ dB. The previous excitation $\mathbf{w}_{\text{pre}}$ is taken as the Chebyshev weight vector with a -30 dB sidelobe attenuation. Table III compares the previous weight $\mathbf{w}_{\text{pre}}$, the resulting $\breve{\mathbf{w}}$ by WORD method, and the ultimate weight vector $\mathbf{w}_{\text{new}}$ of the proposed algorithm. It can be checked that $|w_{\text{new},n}| = |w_{\text{pre},n}|$, $n = 1, \ldots, N$, and the resulting phase values of $\mathbf{w}_{\text{new}}$ are similar to those of $\breve{\mathbf{w}}$. In this case, we obtain $\psi_c = 0.7691$. Fig. 10 depicts the previous pattern and the resulting beampatterns of different approaches. One can observe that all the three methods can adjust the single-point response as desired in this scenario. In other words, the resulting D's are all zeros. When testing the metric E, we have $E = 0$ for SDR method and the proposed one and obtain $E = 0.0088$ for the CR method. This result indicates that the ultimate amplitude excitations of CR may be different from those of the previous weight $\mathbf{w}_{\text{pre}}$, with the possible reason of the relaxation operation. In addition, the execution time of the proposed algorithm is 0.06 s, which is much shorter than those of SDR (41.03 s) and CR (14.55 s).

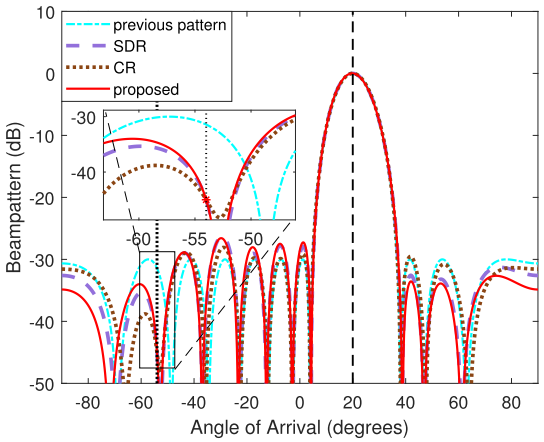

Fig. 10. Resulting patterns starting from a Chebyshev weight.

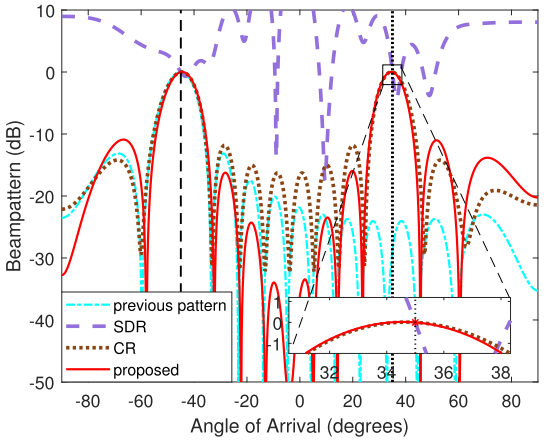

Fig. 11. Resulting patterns of phase-only two-beam synthesis.

B. Phase-Only Two-Beam Synthesis

To show that our algorithm is applicable when the response level at θ_c needs to be elevated, we carry out the second example by considering a 16-element ULA with 0.4 wavelength spacing. The elements are isotropic. In this case, we take $\theta_0 = -45°$ and preassign $\mathbf{w}_{\text{pre}} = \mathbf{a}(\theta_0)$. Suppose that there appears a burst signal at $\theta_c = 35°$. To fulfill the burst signal reception, we take the desired level at θ_c as $\rho_c = 0$ dB and expect to shape a two-beam pattern (pointing to θ_0 and θ_c, respectively) with the phase-only constraint. Fig. 11 presents the resulting beampatterns of different methods. One can see clearly that the pattern of the SDR approach is distorted, although the response level at θ_c has been precisely adjusted as desired. Both the CR approach and the proposed one succeed to synthesize the desirable two-beam patterns as depicted in Fig. 11. However, the ultimate weight of CR method has different entry moduli from those of the previous weight $\mathbf{w}_{\text{pre}}$. In fact, we have $E = 0.5195$ for the CR method and obtain $E = 0$ for the proposed one. The running time of our algorithm is 0.01 s, which is much shorter than those of CR (0.67 s) and SDR (2.59 s). Thus, the effectiveness and superiority of the proposed algorithm can be verified for the burst signal reception.

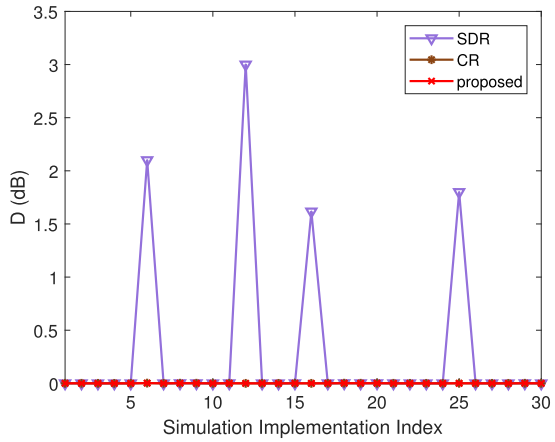

Fig. 12. Curves of D versus the implementation index.

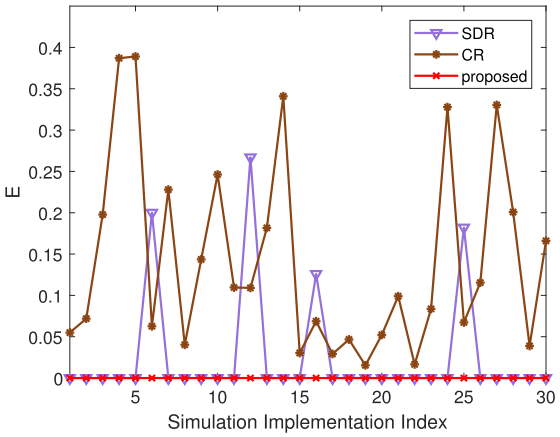

Fig. 13. Curves of E versus the implementation index.

C. Further Investigation With Randomized Configuration

To show that our algorithm behaves well not only under carefully chosen array configurations, we carry out the test by randomly selecting the element number and positions. We fix the beam axis as $\theta_0 = -40°$ and prescribe the controlled angle as $\theta_c = 25°$. In this case, we consider a linear array with isotropic elements. We conduct Monte Carlo simulation with 30 realizations. The element number N in each realization is randomly selected as a positive integer from 12 to 20. The element space between two adjacent sensors is distributed uniformly in the range $[0.4\lambda, 0.6\lambda]$. In addition, the desired level ρ_c is uniformly selected in the range $[-50$ dB, 0 dB$]$. The previous weight is taken as $\mathbf{w}_{\text{pre}} = \mathbf{a}(\theta_0)$.

With the above settings, we depict the curves of metrics D and E versus the implementation index in Fig. 12 and Fig. 13, respectively. We can see from Fig. 12 that the SDR method may not precisely adjust the response level at θ_c to the desired level ρ_c. Moreover, in most cases, the obtained weight vectors of SDR and CR have different entry moduli from those of the previous weights, as presented by the resulting E in Fig. 13. As a result, SDR and CR may fail to realize phase-only control with randomized settings. As aforementioned, the possible reasons are the relaxation operations that may change the original problems. For our algorithm, we have $D = E = 0$ in each realization. Therefore, the proposed algorithm behaves well under the circumstances of carefully chosen array configurations.

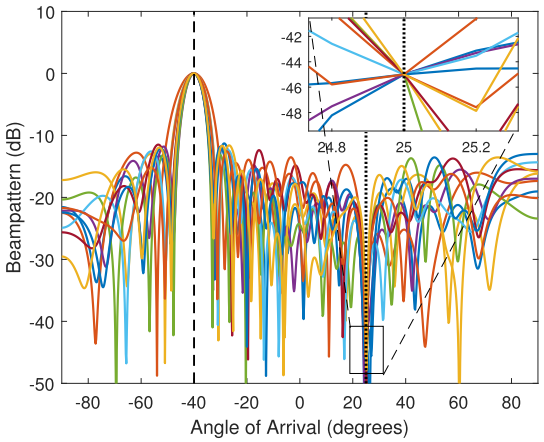

Fig. 14. Resulting patterns of the proposed algorithm for ten randomly generated configurations.

We next present the radiation patterns of the proposed algorithm with randomized configurations. In this case, we fix the desired level ρ_c as -45 dB. Fig. 14 presents the resulting beampatterns of ten realizations with different element numbers and positions. One can see from Fig. 14 that the devised algorithm can precisely adjust the response level at θ_c to the desired level in each simulation realization. Moreover, Fig. 14 shows that the resulting sidelobes of our algorithm are satisfactory with no occurrence of pattern distortion. This further validates that the proposed algorithm behaves well under the circumstances of randomized array configurations.

IV. Conclusion

In this paper, we have presented a geometric approach to fast array response adjustment with phase-only constraint. The devised method can precisely and rapidly adjust the response of a given point with the phase-only constraint, starting from any preassigned weight vector. In our algorithm, the single-point phase-only array response adjustment is reformulated geometrically as a polygon construction problem, which can be further solved by edge rotation. To avoid undesirable pattern distortion and result of less pattern variations at the uncontrolled region, an effective and analytical phase determination approach has been proposed with attractive computational complexity. Representative simulations have been presented to verify the effectiveness and superiority of the proposed algorithm under various scenarios. The limitation of our algorithm is that it can only adjust one-point response as desired and fails to adjust multiple points with phase-only restriction. With the same concept, we may consider the multipoint phase-only array response adjustment in our further study.

Appendix A
Proof of Proposition 1

To prove Proposition 1, we first study the nonnullity of $\mathbb{X}_2$. Suppose that (11) is true, it can be found that

$$d_1 - d_2 \le d_1 + d_2 \tag{66a}$$

$$d_1 - d_2 \leq \sum_{k=3}^{N} d_k \tag{66b}$$

$$\max\left\{0, d_3 - \sum_{k=4}^{N} d_k\right\} \leq \min\left\{d_1 + d_2, \sum_{k=3}^{N} d_k\right\} \tag{66c}$$

where the inequality $d_1 \geq d_2 \geq \ldots \geq d_N > 0$ is utilized. According to the expression of $\mathbb{X}_2$ in (22), one can further know that $x_{2,\min} \leq x_{2,\max}$. Thus, $\mathbb{X}_2$ is nonempty if $d_1 \leq Q(2, N)$ is satisfied.

In the following derivations, the subscript i can be selected as $3, \ldots, N-2$. In this case, we can first obtain the following inequality:

$$|x_{i-1} - d_i| \leq x_{i-1} + d_i. \tag{67}$$

From $d_1 \geq d_2 \geq \ldots \geq d_N > 0$, one can readily obtain that

$$\max\left\{0, d_{i+1} - \sum_{k=i+2}^{N} d_k\right\} \leq \min\left\{x_{i-1} + d_i, \sum_{k=i+1}^{N} d_k\right\}.$$

Recalling the formulation of $\mathbb{X}_i$ in (31) and combining (67), one can see that the set $\mathbb{X}_i$ is nonempty if

$$|x_{i-1} - d_i| \leq \sum_{k=i+1}^{N} d_k. \tag{68}$$

Suppose that $x_{i-1} \in \mathbb{X}_{i-1}$, one can further learn that x_{i-1}, $d_i, \ldots, d_N$ can form a polygon. Thus, one of the following two conditions is satisfied, i.e.,

$$x_{i-1} \leq d_i \leq x_{i-1} + \sum_{k=i+1}^{N} d_k \tag{69}$$

or

$$d_i < x_i \leq \sum_{k=i}^{N} d_k. \tag{70}$$

Since both (69) and (70) can indicate (68), we know that $\mathbb{X}_i$ is nonempty provided that $x_{i-1} \in \mathbb{X}_{i-1}$. This completes the derivation of Proposition 1.

ACKNOWLEDGMENT

The authors would like to thank the editor and the anonymous reviewers for their valuable comments and suggestions.

REFERENCES

[1] X. Zhang, Z. He, B. Liao, X. Zhang, Y. Yang, and S. Shi, "A fast method for array response adjustment with phase-only constraint," in *Proc. IEEE Radar Conf.*, Apr. 2019, pp. 1–5. [Online]. Available: https://arxiv.org/abs/1811.06030

[2] O. Bucci, G. D'Elia, G. Mazzarella, and G. Panariello, "Antenna pattern synthesis: A new general approach," *Proc. IEEE*, vol. 82, no. 3, pp. 358–371, Mar. 1994.

[3] S. E. Nai, W. Ser, Z. L. Yu, and H. Chen, "Beampattern synthesis for linear and planar arrays with antenna selection by convex optimization," *IEEE Trans. Antennas Propag.*, vol. 58, no. 12, pp. 3923–3930, Dec. 2010.

[4] C.-C. Tseng and L. J. Griffiths, "A simple algorithm to achieve desired patterns for arbitrary arrays," *IEEE Trans. Signal Process.*, vol. 40, no. 11, pp. 2737–2746, Nov. 1992.

[5] C.-Y. Tseng and L. J. Griffiths, "A unified approach to the design of linear constraints in minimum variance adaptive beamformers," *IEEE Trans. Antennas Propag.*, vol. 40, no. 12, pp. 1533–1542, Dec. 1992.

[6] X. Zhang, Z. He, B. Liao, Y. Yang, J. Zhang, and X. Zhang, "Flexible array response control via oblique projection," *IEEE Trans. Signal Process.*, vol. 67, no. 12, pp. 3126–3139, Jun. 2019.

[7] X. Zhang, Z. He, B. Liao, X. Zhang, Z. Cheng, and Y. Lu, "A^{2}RC: An accurate array response control algorithm for pattern synthesis," *IEEE Trans. Signal Process.*, vol. 65, no. 7, pp. 1810–1824, Apr. 2017.

[8] X. Zhang, Z. He, B. Liao, X. Zhang, and W. Peng, "Pattern synthesis with multipoint accurate array response control," *IEEE Trans. Antennas Propag.*, vol. 65, no. 8, pp. 4075–4088, Aug. 2017.

[9] X. Zhang, Z. He, B. Liao, X. Zhang, and W. Peng, "Pattern synthesis for arbitrary arrays via weight vector orthogonal decomposition," *IEEE Trans. Signal Process.*, vol. 66, no. 5, pp. 1286–1299, Mar. 2018.

[10] A. D. Khzmalyan and A. S. Kondratiev, "The phase-only shaping and adaptive nulling of an amplitude pattern," *IEEE Trans. Antennas Propag.*, vol. 51, no. 2, pp. 264–272, Feb. 2003.

[11] G. Buttazzoni and R. Vescovo, "Power synthesis for reconfigurable arrays by phase-only control with simultaneous dynamic range ratio and near-field reduction," *IEEE Trans. Antennas Propag.*, vol. 60, no. 2, pp. 1161–1165, Feb. 2012.

[12] R. M. Davis, "Phase-only LMS and perturbation adaptive algorithms," *IEEE Trans. Aerosp. Electron. Syst.*, vol. 34, no. 1, pp. 169–178, Jan. 1998.

[13] A. F. Morabito, A. Massa, P. Rocca, and T. Isernia, "An effective approach to the synthesis of phase-only reconfigurable linear arrays," *IEEE Trans. Antennas Propag.*, vol. 60, no. 8, pp. 3622–3631, Aug. 2012.

[14] O. M. Bucci and G. D'Elia, "Power synthesis of reconfigurable conformal arrays with phase-only control," *IET Microw., Antennas Propag.*, vol. 145, no. 1, pp. 131–136, Feb. 1998.

[15] J. F. DeFord and O. P. Gandhi, "Phase-only synthesis of minimum peak sidelobe patterns for linear and planar arrays," *IEEE Trans. Antennas Propag.*, vol. AP-36, no. 2, pp. 191–201, Feb. 1988.

[16] G. M. Kautz, "Phase-only shaped beam synthesis via technique of approximated beam addition," *IEEE Trans. Antennas Propag.*, vol. 47, no. 5, pp. 887–894, May 1999.

[17] W.-S. Choi and T. K. Sarkar, "Phase-only adaptive processing based on a direct data domain least squares approach using the conjugate gradient method," *IEEE Trans. Antennas Propag.*, vol. 52, no. 12, pp. 3265–3272, Dec. 2004.

[18] A. F. Morabito and P. Rocca, "Reducing the number of elements in phase-only reconfigurable arrays generating sum and difference patterns," *IEEE Antennas Wireless Propag. Lett.*, vol. 14, pp. 1338–1341, 2015.

[19] R. Kadlimatti and P. V. Parimi, "Phased arrays using odd phase distribution of the radiating elements," *IEEE Antennas Wireless Propag. Lett.*, vol. 18, no. 5, pp. 891–895, May 2019.

[20] R. Vescovo, "Reconfigurability and beam scanning with phase-only control for antenna arrays," *IEEE Trans. Antennas Propag.*, vol. 56, no. 6, pp. 1555–1565, Jun. 2008.

[21] O. M. Bucci, G. Mazzarella, and G. Panariello, "Reconfigurable arrays by phase-only control," *IEEE Trans. Antennas Propag.*, vol. 39, no. 7, pp. 919–925, Jul. 1991.

[22] A. Trastoy, F. Ares, and E. Moreno, "Phase-only control of antenna sum and shaped patterns through null perturbation," *IEEE Antennas Propag. Mag.*, vol. 43, no. 6, pp. 45–54, Dec. 2001.

[23] K. Hirasawa, "The application of a biquadratic programming method to phase only optimization of antenna arrays," *IEEE Trans. Antennas Propag.*, vol. AP-36, no. 11, pp. 1545–1550, Nov. 1988.

[24] H. Lebret and S. Boyd, "Antenna array pattern synthesis via convex optimization," *IEEE Trans. Signal Process.*, vol. 45, no. 3, pp. 526–532, Mar. 1997.

[25] B. Fuchs, "Application of convex relaxation to array synthesis problems," *IEEE Trans. Antennas Propag.*, vol. 62, no. 2, pp. 634–640, Feb. 2014.

[26] Z.-Q. Luo, W.-K. Ma, A. M.-C. So, Y. Ye, and S. Zhang, "Semidefinite relaxation of quadratic optimization problems," *IEEE Signal Process. Mag.*, vol. 27, no. 3, pp. 20–34, May 2010.

[27] P. Cao, J. S. Thompson, and H. Haas, "Constant modulus shaped beam synthesis via convex relaxation," *IEEE Antennas Wireless Propag. Lett.*, vol. 16, pp. 617–620, 2017.

[28] C. Baird and G. Rassweiler, "Adaptive sidelobe nulling using digitally controlled phase-shifters," *IEEE Trans. Antennas Propag.*, vol. AP-24, no. 5, pp. 638–649, Sep. 1976.

[29] H. Steyskal, "Simple method for pattern nulling by phase perturbation," *IEEE Trans. Antennas Propag.*, vol. AP-31, no. 1, pp. 163–166, Jan. 1983.

[30] R. A. Shore, "Nulling a symmetric pattern location with phase-only weight control," *IEEE Trans. Antennas Propag.*, vol. 32, no. 5, pp. 530–533, May 1984.
[31] P. J. Kajenski, "Phase only antenna pattern notching via a semidefinite programming relaxation," *IEEE Trans. Antennas Propag.*, vol. 60, no. 5, pp. 2562–2565, May 2012.
[32] R. Ghayoula, N. Fadlallah, A. Gharsallah, and M. Rammal, "Phase-only adaptive nulling with neural networks for antenna array synthesis," *IET Microw., Antennas Propag.*, vol. 3, no. 1, pp. 154–163, 2009.
[33] R. L. Haupt, "Phase-only adaptive nulling with a genetic algorithm," *IEEE Trans. Antennas Propag.*, vol. 45, no. 6, pp. 1009–1015, Jun. 1997.
[34] T. Van Luyen and T. V. B. Giang, "Interference suppression of ULA antennas by phase-only control using bat algorithm," *IEEE Antennas Wireless Propag. Lett.*, vol. 16, pp. 3038–3042, 2017.
[35] R. A. Monzingo and T. W. Miller, *Introduction to Adaptive Antennas*. New York, NY, USA: Wiley, 1980.
[36] R. L. Haupt, "Adaptive nulling in monopulse antennas," *IEEE Trans. Antennas Propag.*, vol. AP-36, no. 2, pp. 202–208, Feb. 1988.
[37] S. T. Smith, "Optimum phase-only adaptive nulling," *IEEE Trans. Signal Process.*, vol. 47, no. 7, pp. 1835–1843, Jul. 1999.
[38] J. Zhang, Y. Huang, J. Wang, B. Ottersten, and L. Yang, "Per-antenna constant envelope precoding and antenna subset selection: A geometric approach," *IEEE Trans. Signal Process.*, vol. 64, no. 23, pp. 6089–6104, Dec. 2016.

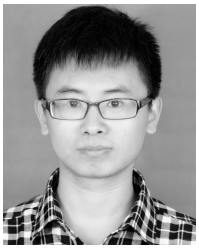

Xuejing Zhang (S'17) was born in Hebei, China. He received the B.S. degree in electrical engineering from Huaqiao University, Xiamen, China, in 2011 and the M.S. degree in signal and information processing from Xidian University, Xi'an, China, in 2014. He is currently pursuing the Ph.D. degree in signal and information processing with the School of Information and Communication Engineering, University of Electronic Science and Technology of China (UESTC), Chengdu, China.

Since 2017, he has been a Visiting Student with the University of Delaware, Newark, DE, USA. His current research interests include array signal processing and wireless communications.

Zishu He (M'11) was born in Sichuan, China, in 1962. He received the B.S., M.S., and Ph.D. degrees in signal and information processing from the University of Electronic Science and Technology of China (UESTC), Chengdu, China, in 1984, 1988, and 2000, respectively.

He is currently a Professor with the School of Information and Communication Engineering, UESTC. His current research interests include array signal processing, digital beam forming, the theory on multiple-input multiple-output (MIMO) communication and MIMO radar, adaptive signal processing, and interference cancellation.

Bin Liao (S'09–M'13–SM'16) received the B.Eng. and M.Eng degrees in electronic engineering from Xidian University, Xian, China, in 2006 and 2009, respectively, and the Ph.D. degree in electronic engineering from The University of Hong Kong, Hong Kong, in 2013.

From 2013 to 2014, he was a Research Assistant with the Department of Electrical and Electronic Engineering, The University of Hong Kong. From 2016 to 2016, he was a Research Scientist with the Department of Electrical and Electronic Engineering, The University of Hong Kong. He is currently an Associate Professor with the Guangdong Key Laboratory of Intelligent Information Processing, Shenzhen University, Shenzhen, China. His current research interests include sensor array processing, adaptive filtering, and convex optimization, with applications to radar, navigation, and communications.

Dr. Liao was a recipient of the Best Paper Award at the 21st International Conference on Digital Signal Processing (2016 DSP) and the 22nd International Conference on Digital Signal Processing (2017 DSP). He is currently an Associate Editor of the IEEE TRANSACTIONS ON AEROSPACE AND ELECTRONIC SYSTEMS, *IET Signal Processing*, *Multidimensional Systems and Signal Processing*, and IEEE ACCESS.

Xuepan Zhang was born in Hebei, China. He received the B.S. and Ph.D. degrees in electrical engineering from the National Laboratory of Radar Signal Processing, Xidian University, Xian, China, in 2010 and 2015, respectively.

He is currently a Principal Investigator with the Qian Xuesen Laboratory of Space Technology, Beijing, China. His current research interests include synthetic aperture radar (SAR), ground moving target indication (GMTI), and deep learning.